



Published in final edited form as:

Cell Host Microbe. 2013 September 11; 14(3): 306–317. doi:10.1016/j.chom.2013.08.013.

Identifying *Yersinia* YopH-targeted signal transduction pathways that impair neutrophil responses during *in vivo* murine infection

Hortensia G. Rolán^{2,1}, Enrique A. Durand^{3,1}, and Joan Meccas^{2,3,4}

²Dept. of Molecular Biology and Microbiology, Tufts University School of Medicine

³Graduate Program in Molecular Microbiology, Sackler School of Biomedical Sciences, Tufts University School of Medicine

Summary

Identifying molecular targets of *Yersinia* virulence effectors, or Yops, during animal infection is challenging because few cells are targeted by Yops in an infected organ and isolating these sparse effector-containing cells is difficult. YopH, a tyrosine phosphatase, is essential for full virulence of *Yersinia*. Investigating the YopH-targeted signal-transduction pathway(s) in neutrophils during infection of a murine host, we find that several host proteins, including the essential signaling adapter SLP-76, are dephosphorylated in the presence of YopH in neutrophils isolated from infected tissues. YopH inactivated PRAM-1/SKAP-HOM and the SLP-76/Vav/PLC 2 signal-transduction axes, leading to an inhibition of calcium response in isolated neutrophils. Consistent with a failure to mount a calcium response, IL-10 production was reduced in neutrophils containing YopH from infected tissues. Finally, a *yopH* mutant survived better in the absence of neutrophils, indicating that neutrophil inactivation by YopH by targeting PRAM-1/SKAP-HOM and SLP-76/Vav/PLC 2 signaling hubs may be critical for *Yersinia* survival.

Introduction

Polymorphonuclear neutrophils (PMNs) migrate rapidly to infected tissues, killing invading bacteria through a variety of mechanisms, which include the production of reactive oxygen intermediates (ROI), phagocytosis, degranulation, and production of neutrophil extracellular traps (NETs) (Nathan, 2006). PMNs also secrete cytokines and chemokines, which modulate additional immune responses either by activating resident immune cells (Geijtenbeek and Gringhuis, 2009), or by suppressing additional inflammation through secretion of IL-10 (Zhang et al., 2009). One strategy bacterial pathogens use to counteract these clearance mechanisms is through the direct delivery of effector proteins into host cells by way of a Type 3 Secretion System (T3SS) (Viboud and Bliska, 2005). The *Yersinia* species are predominantly extracellular bacteria that depend on their T3SS for productive infection (Viboud and Bliska, 2005). All three *Yersinia* species that are pathogenic in humans, *Yersinia pseudotuberculosis* (*Yptb*), *Y. enterocolitica* and *Y. pestis*, target PMNs, macrophages and dendritic cells for translocation of their effector proteins, called Yops, (Durand et al., 2010; Koberle et al., 2009; Marketon et al., 2005). This suggests that Yops

© 2013 Elsevier Inc. All rights reserved.

⁴Corresponding author: Dept of Molecular Biology and Microbiology, Tufts University School of Medicine, 136 Harrison Ave, Boston MA 02111, Phone 617-636-2742, FAX: 617-636-0337, joan.meccas@tufts.edu.

¹These authors contributed equally to this work

Publisher's Disclaimer: This is a PDF file of an unedited manuscript that has been accepted for publication. As a service to our customers we are providing this early version of the manuscript. The manuscript will undergo copyediting, typesetting, and review of the resulting proof before it is published in its final citable form. Please note that during the production process errors may be discovered which could affect the content, and all legal disclaimers that apply to the journal pertain.

are critical for inactivating PMNs in tissue infection and highlights the importance of studying their functions in PMNs. Yop delivery by the T3SS requires that *Yersinia* bind tightly to host cells (Grosdent et al., 2002). This tight association could render *Yersinia* susceptible to capture and killing by PMNs through phagocytosis and/or by NETs (Casutt-Meyer et al., 2010; Grosdent et al., 2002). Collectively, Yops are presumed to block these killing mechanisms and inactivate PMNs in tissue infection (Andersson et al., 1999; Grosdent et al., 2002; Spinner et al., 2008), however the precise mechanisms used to inactivate PMNs in tissue infection is not known.

YopH, a tyrosine phosphatase, is critical for virulence of *Yersinia* and has been studied extensively in a variety of cell culture systems and in animal infection models (Black et al., 1998; Deleuil et al., 2003; Logsdon and Meccas, 2003; Persson et al., 1997; Yuan et al., 2005). In isolated human PMNs, YopH inhibits phagocytosis and calcium flux (Andersson et al., 1999; Grosdent et al., 2002; Spinner et al., 2008) but it is not known which proteins YopH targets to prevent these activities in PMNs. Two main classes of proteins, tyrosine kinases and their adapters, have been identified as YopH substrates in various cell types. In some cases, a substrate-trapping YopH mutant co-precipitates with these substrates suggesting that they may be direct targets of YopH (Black and Bliska, 1997; Black et al., 2000; Black et al., 1998; Gerke et al., 2005; Hamid et al., 1999); however, since many of these proteins act in complexes, direct targets can be difficult to discern. In epithelial cells, the adapters p130Cas and paxillin (Black et al., 1998) interact with YopH. In macrophages, the adapters ADAP, SKAP-HOM and the tyrosine kinase FAK (Hamid et al., 1999; Persson et al., 1997) associate with a substrate trapping mutant. In T cells, the tyrosine kinases, Lck and ZAP-70, and the adapters SLP-76 and LAT are dephosphorylated in the presence of YopH (Alonso et al., 2004; Gerke et al., 2005).

Many of these YopH targets are found or have homologs in PMNs, and might be targets of YopH in PMNs during animal infection. However, until recently, it has been technically challenging to identify the molecular targets of Yops during animal infection because there were no good methods for isolating the cells that contain effectors and the number of non-targeted cells vastly exceeds the number of Yop-injected cells in an infected organ. Thus, the effect of a Yop can be masked or diluted when examining the whole population of a particular cell type from an infected tissue. Using the TEM system (Durand et al., 2010), we show that the PRAM-1/SKAP-HOM and SLP-76 signal-transduction pathway(s) is dephosphorylated in the presence of YopH in PMNs, thus identifying a molecular target of a T3SS effector in the context of animal infection.

Results

Depletion of PMNs permits growth of a $\Delta yopH$ mutant during co-infection with wild-type *Yptb*

Because YopH is critical for *Yptb* survival in the mouse (Bliska et al., 1991; Logsdon and Meccas, 2003) and PMNs are important targets of Yop translocation (Durand et al., 2010; Koberle et al., 2009; Marketon et al., 2005), we hypothesized that YopH inactivates PMNs during *Yptb* infection. To test this hypothesis, mice were depleted of PMNs with either antibody to Ly6G (1A8), which depletes only PMNs, or antibody to Gr-1 (RB6-8C5), which depletes both PMNs and inflammatory monocytes (iMo) (Daley et al., 2008). Mice were injected intravenously (IV) with an equal mixture of WT *Yptb* and a *yopH* mutant. Three days post infection (p.i.), PMN levels in the spleen were reduced by 85%–99%, as measured by FACS (Fig 1A). Strikingly, the *yopH* strain competed better in the spleen (Fig 1B) and liver (Fig 1C) relative to the WT strain in the PMN-depleted mice than in control mice. This suggests that YopH is critical for inactivating a specific bactericidal function of PMNs to enhance survival of *Yptb*. The total number of bacteria in these organs were similar in both

groups of mice (Fig 1D–E), suggesting that at this time point, *Yptb* efficiently disarms PMNs.

YopH dephosphorylates several proteins in splenic PMNs

To understand how YopH inactivates PMNs in infected animals, we investigated the molecular target(s) of YopH in PMNs during animal infection. The TEM system can be used to identify and isolate PMNs that contain Yops in an animal because TEM^{POS} cells also contain other Yops (Durand et al., 2010). An ETEM gene fusion was introduced into WT and *yopH* strains (Harmon et al., 2010). Cells that are translocated with ETEM and incubated with CCF4-AM fluoresce blue (TEM^{POS}), whereas cells lacking TEM and incubated with CCF4 fluoresce green (TEM^{NEG}). Surface staining with cell-type specific antibodies allows for the isolation of different types of cells within TEM^{POS} and TEM^{NEG} populations by FACS.

Mice were infected IV with 200 CFU of WT-ETEM or 2000 CFU *yopH*-ETEM so that equivalent numbers of *Yptb* were recovered. Spleens were harvested and TEM^{POS}Ly6G⁺ PMNs were separated from TEM^{NEG}Ly6G⁺ PMNs by FACS (Fig 2A). Day 5 was chosen because the greatest number of TEM^{POS} cells was recovered. Analysis of splenic PMN lysates by Western blot with a phospho-tyrosine antibody revealed that at least 5 proteins with molecular weights of ~200kDa, ~160kDa, ~70kDa, ~55kDa and ~35kDa had decreased levels of phosphorylation in the presence of YopH compared to their levels of phosphorylation in the absence of YopH (Fig 2B–C and Fig S1A–B). This result suggests that YopH has multiple targets or that YopH dephosphorylates one protein in a signal-transduction pathway, which affects the phosphorylation state of additional proteins in that pathway.

To determine if the spectrum of dephosphorylated bands was similar in PMNs isolated from bone marrow (BMPMNs), BMPMNs were infected with WT or *yopH* for 30 min at MOI 50:1 (Fig 2D–E and Fig S1B). Again several proteins with molecular weights of ~160kDa, ~120kDa, ~70kDa, ~55kDa and ~35kDa had reduced levels of phosphorylation after infection with WT compared to those BMPMNs infected with *yopH* (Fig 2B–C), suggesting that YopH targets many of the same proteins in isolated BMPMNs as it does in PMNs isolated from infected animals. More noticeable dephosphorylation was observed in isolated BMPMNs versus PMNs isolated from infected spleens, which is likely the result of a more synchronous infection of BMPMNs and/or the fact that BMPMNs were exposed to a greater MOI of *Yptb*.

SLP-76, but not paxillin, is dephosphorylated in the presence of YopH in PMNs from infected spleens

We first focused on testing whether the ~70 kDa band, which had a strong YopH-dependent dephosphorylation phenotype in both conditions (Fig 2B–E), represented one of the known ~70kDa YopH targets, SLP-76 or paxillin (Black et al., 1998; Gerke et al., 2005). In PMNs, SLP-76 (76 kDa) is involved in signal-transduction events important for activating ROS (Newbrough et al., 2003), while paxillin (68 kDa) is involved in actin dynamics leading to phagocytosis and cell movement (Schaller, 2001). TEM^{POS} Gr1⁺CD11b⁺ cells, which include both PMNs and iMO, were isolated from mice infected for 5 days with either WT-ETEM or *yopH*-ETEM and analyzed by Western blot for SLP-76 phosphorylation at residue Y128. The level of phospho-Y128-SLP-76 in mice infected with WT-ETEM was drastically reduced compared to its level in mice infected with *yopH*-ETEM (Fig 3A). To confirm that phosphorylation of SLP-76 was reduced in PMNs in the presence of YopH, BMPMNs were infected with WT *Yptb* or *yopH* for 5 minutes. Proteins from BMPMN lysates were immunoprecipitated with SLP-76 antibody and the precipitated complexes were

probed with anti-SLP-76 phospho-Y128 (Fig 3B). Consistent with our analysis of PMNs recovered from infected mice, SLP-76 was dephosphorylated in a YopH-dependent manner. Combined, these results indicate that the SLP-76 signal-transduction pathway is targeted for dephosphorylation by YopH in PMNs during mouse infection and in BMPMNs.

Next we tested whether paxillin was dephosphorylated in a YopH-dependent manner in BMPMNs. No dephosphorylation of paxillin Y-118 was observed in these cells regardless of the presence or absence of YopH (Fig 3C). To confirm that dephosphorylation of paxillin, a well-established target of YopH in epithelial cells (Black et al., 1998), was detectable with this antibody, HEp-2 cells and BMPMNs were infected with either WT-E TEM or *yopH*-E TEM and analyzed by Western blot (Fig 3D). As expected, YopH-dependent dephosphorylation of paxillin was observed in HEp2 cells, suggesting that paxillin is not a major target of YopH in PMNs during infection.

In PMNs, SKAP-HOM and PRAM-1, but not Syk or ADAP, have reduced levels of phosphorylation in the presence of YopH

SLP-76 is critical for transducing signaling events downstream of both immunoreceptors and integrin receptors (Geijtenbeek and Gringhuis, 2009; Newbrough et al., 2003). Therefore, we investigated whether there was a YopH-dependent change in phosphorylation status of proteins involved in transmitting signals from either of these receptors upstream of SLP-76 (Fig S2). In PMNs, immunoreceptors transmit signals to SLP-76 through the adapter protein, Syk (72kDa) (Newbrough et al., 2003). A homolog of Syk, ZAP-70, has reduced levels of phosphorylation in the presence of YopH in Jurkat T cells (Gerke et al., 2005; Newbrough et al., 2003). To determine whether Syk is targeted by YopH, TEM^{pos}Gr1⁺CD11b⁺ and TEM^{neg}Gr1⁺CD11b⁺ cells (both PMNs and iMOs) were harvested from spleens of mice infected with either WT-E TEM or *yopH*-E TEM (4A). Western blot analysis revealed that the level of phospho-Y352-Syk in TEM^{pos}Gr1⁺CD11b⁺ cells infected with WT-E TEM was comparable to its level in TEM^{pos}Gr1⁺CD11b⁺ cells infected with *yopH*-E TEM. This result suggests that the Y352 residue of Syk is not a target of YopH in these cells. Phosphorylation of Syk at position Y352 leads to a conformational change in the Syk kinase domain from a closed to an open configuration (Kulathu et al., 2009). Syk then autophosphorylates the tyrosines in its activation loop at positions 525/526, which results in recruitment of LAT and the propagation of signaling through SLP-76 (Carsetti et al., 2009). Because we observed stronger dephosphorylation signals in isolated BMPMNs than in PMNs isolated from spleens after mouse infection (Fig 2D), we assessed the phosphorylation state of Syk in these cells following infection. Western blot analysis of isolated BMPMNs infected with WT or *yopH* for 5 or 30 minutes showed that the levels of phosphorylation at Y352 and Y535/536 in Syk were not altered in the presence of YopH (Fig 4B). Combined these results suggest that Syk is not a major target of YopH in PMNs.

Next, we investigated whether proteins relaying signals from integrin receptors were dephosphorylated in PMNs in the presence of YopH (Fig S2). ADAP (130 kDa) is a known target of YopH in macrophages (Hamid et al., 1999) that signals downstream of integrin receptors. As the molecular weight of ADAP is within the range of the ~120 kDa band that was dephosphorylated in the presence of YopH in BMPMNs (Fig 2D–E, Fig S1C), we tested whether YopH dephosphorylates ADAP in PMNs. BMPMNs were infected with WT *Yptb* or *yopH* for 30 minutes. Proteins from lysates were immunoprecipitated with ADAP antibodies and the precipitated complexes were analyzed by Western blot with anti-phosphotyrosine antibody (Fig 4C). Surprisingly, ADAP was not dephosphorylated in BMPMNs, although as previously reported (Hamid et al., 1999), ADAP was dephosphorylated in a YopH-dependent manner in J774 cells (Fig 4C). Notably, the total levels of ADAP in BMPMNs were lower when compared to its levels in other lymphoid cell types, such as J774 macrophages and Jurkat T cells (Fig S3). These results suggest that

ADAP is not a major target of YopH in PMNs or that it is only transiently dephosphorylated by YopH and not detected during the time-course of these experiments.

ADAP has a homolog, PRAM-1 (100kDa) that is highly expressed in myeloid cells (Clemens et al., 2004) including PMNs (Fig S3). PRAM-1 has been implicated in integrin signaling in PMNs (Clemens et al., 2004) and interacts with some of the same partners as does ADAP, including SLP-76 and SKAP-HOM (Moog-Lutz et al., 2001). To test whether PRAM-1 was dephosphorylated in PMNs in a YopH-dependent manner, PRAM-1 was immunoprecipitated from BMPMNs infected with WT *Yptb* or *yopH* and the precipitated complexes were analyzed by Western blot with anti-phosphotyrosine antibody (Fig 4D). In contrast to ADAP, PRAM-1 was dephosphorylated in a YopH-dependent manner in BMPMNs, suggesting that YopH may directly target PRAM-1 and/or may target another protein that relays signals from integrins through PRAM-1 to SLP-76.

We next examined whether SKAP-HOM (55kDa) was dephosphorylated after infection with *Yptb*, because PRAM-1 associates with SKAP-HOM (Moog-Lutz et al., 2001), SKAP-HOM has been identified as a YopH target in macrophages (Black et al., 2000), and a band of approximately 55kDa was dephosphorylated in a YopH-dependent manner in PMNs (Fig 2B–2E). Immunoprecipitation followed by Western blot with anti-phosphotyrosine antibody indicated that SKAP-HOM was dephosphorylated in a YopH-dependent manner (Fig 4E). In summary, these results indicate that YopH can block signals downstream of integrin receptors and prior to SLP-76 activation. YopH may dephosphorylate multiple proteins or the dephosphorylation of PRAM-1 and/or SKAP-HOM may result in the low levels of phosphorylation of SLP-76.

YopH targets the SLP-76/Vav/PLC γ 2 signaling axis and inhibits calcium flux in PMNs

Phosphorylation of SLP-76 occurs at three sites, Y112, Y128 and Y145, and each phosphorylation site recruits and activates sets of effectors that can then direct host responses (Jordan and Koretzky, 2010). To identify the specific SLP-76 tyrosine residue(s) that were not phosphorylated in the presence of YopH, we infected BMPMNs for 5 or 30 minutes with WT or *yopH* and probed the cell lysates with antibodies that specifically recognize phosphorylated Y112, Y128 or Y145 in SLP-76. At 5 and 30 min post-infection, SLP-76 tyrosine residues, 112 and 128, but not 145 were dephosphorylated in a YopH-dependent manner (Fig 5A). Thus, YopH prevents high levels of phosphorylation at 2 of 3 sites in SLP-76, which should abrogate signal-transduction cascades downstream of SLP-76 in PMNs.

To investigate if YopH affects the activation of downstream effectors of SLP-76, the phosphorylation states of Vav and PLC 2 were examined in BMPMNs. Five minutes after infection with *yopH*-TEM, both Vav and PLC 2 were clearly phosphorylated indicating that binding of *Yptb* stimulated their phosphorylation (Fig 5A). However, neither was phosphorylated after infection with WT-ETEM (Fig 5A). In PMNs the Vav/PLC 2 signaling cascade induces a release of intracellular calcium within minutes after receptor stimulation and/or infection (Graham et al., 2007). Previous work has shown that YopH blocks bacterial contact-induced immediate-early Ca²⁺ spikes in human PMNs (Andersson et al., 1999), although the mechanism for this phenotype is not understood. To determine whether the disruption of the Vav/PLC 2 pathway by YopH inhibited calcium responses in murine PMNs, we measured the intracellular calcium concentration of BMPMNs following infection with *Yptb*. Ca²⁺ fluxes were observed in BMPMNs infected with *yopH* but not WT (Fig 5B) indicating that YopH is required to block calcium fluxes in mouse PMNs. When BMPMNs were exposed to U73122, an inhibitor of PLC, and then infected with *yopH*, no Ca²⁺ fluxes were observed indicating that activation of PLC was critical for the calcium flux triggered by *yopH* infection (Fig 5C). Calcium fluxes were restored when

BMPMNs were exposed to U73343, an U73122 analogue that does not target PLC, and infected with *yopH* (Fig 5C). Combined, these results suggest that the lack of phosphorylation at Y112 and Y128 at SLP-76 prevented activation and phosphorylation of Vav and PLC 2, altering functions of the SLP-76 complex such that it is unable to induce calcium flux and mount subsequent bactericidal events.

YopH inhibits IL-10 production in PMNs during infection

While many signaling events downstream of SLP-76, including calcium flux, are transient and difficult to observe during animal infections, cytokine production can be a longer-lasting consequence of immune cell activation. In leukocytes, calcium flux triggers activation of NF-AT, which in turn increases transcription of IL-10 (Hogan et al., 2003; Lee et al., 2009). Because PMNs are a major producer of IL-10 in infected tissues (Zhang et al., 2009), we hypothesized that YopH would block transcription of IL-10 in YopH-injected PMNs isolated from infected mice. mRNA from TEM^{pos}Ly6G⁺ PMNs of mice infected for 5 days with *yopH*-E-TEM (Fig 6A–B) had significantly more IL-10 transcript levels than TEM^{pos}Ly6G⁺ cells containing YopH or than TEM^{neg}Ly6G⁺ PMNs (Fig 6B). Moreover, intracellular IL-10 protein levels in TEM^{pos}Gr1⁺CD11b⁺ PMNs and iMO isolated from mice infected for 5 days with *yopH*-E-TEM were significantly higher than TEM^{pos}Gr1⁺CD11b⁺ cells from mice infected with the WT-E-TEM (Fig S4A). These results indicate that in the absence of YopH, *Yptb* infection caused an increase IL-10 transcription and protein levels in injected PMNs. However, translocated YopH blocked this response. TNF- mRNA and protein levels were elevated in TEM^{pos}Ly6G⁺ cells infected either with WT or *yopH* (Fig 6C and Fig S4B) indicating that YopH does not dampen all cytokine production at this time point.

Since YopH prevents phagocytosis by PMNs (Grosdent et al., 2002), it was possible that the increase in IL-10 in PMNs from mice infected with *yopH*-E-TEM was due to a greater number of TEM^{pos} PMNs containing *Yptb* which may trigger more IL-10 production. To investigate this possibility, mice were infected with a *yopE* mutant, *yopE*-E-TEM, which also prevents phagocytosis by PMNs (Grosdent et al., 2002). The levels of IL-10 mRNA in TEM^{pos} PMNs isolated from *yopE*-E-TEM infected mice were comparable to those found in PMNs from WT-E-TEM-infected mice and significantly lower than those found in *yopH*-E-TEM-infected mice (Fig 6B). This result supports the idea that YopH suppresses IL-10 expression in PMNs. Next, the levels of phagocytosed WT, *yopH* or *yopE* mutants were assessed using a gentamicin protection assay on single cell suspensions of spleens from infected mice. Equivalent numbers of WT, *yopH*-E-TEM and *yopE*-E-TEM were recovered from spleens and were protected from gentamicin (Fig S4C–D). Thus, either all strains were internalized at the same efficiency or the mutants were internalized at higher levels but did not survive. Finally, we determined whether the internalized viable WT *Yptb* were detected in TEM^{pos} or TEM^{neg} cells. In 5/7 mice no *Yptb* were recovered TEM^{pos} cells while low but detectable levels were recovered in TEM^{neg} cells (Fig S4E–F). Since the number of TEM^{neg} cells vastly exceeds the number of TEM^{pos} cells and we collected the majority of TEM^{pos} cells, most viable *Yptb* resided within TEM^{neg} cells. The finding that TEM^{pos} cells do not contain live *Yptb* suggests that differences between TEM^{pos} cells from mice infected with different mutants are likely due to the specific effectors within these cells.

To confirm that calcium flux is critical for IL-10 production in PMNs during *Yptb* infection, chemicals that block calcium flux, BAPTA-AM, 2-APB or EGTA, were added to BMPMNs. BMPMNs were then infected with *Yptb* strains lacking 5 effector Yops, 5, or 5 strains in which YopH or YopE were expressed from an arabinose-inducible promoter. Supernatants were collected and IL-10 levels were determined (Fig 6D and Fig S4G). In the absence of calcium flux inhibitors, significantly higher levels of IL-10 were detected in

supernatants of BMPMNs infected with $\Delta 5$ and $\Delta 5+pYopE$ compared to $\Delta 5+pYopH$, confirming that the presence of YopH is sufficient to block IL-10 production after $\Delta 5$ infection. When calcium flux was blocked, IL-10 levels produced by $\Delta 5$ and $\Delta 5+pYopE$ dropped to the similar levels as those found in uninfected controls and $\Delta 5+pYopH$ infected cells, indicating that calcium flux was required for IL-10 production. LDH release was measured to determine if IL-10 release was either due to or blocked by cell death of BMPMNs (Fig 6E and Fig S4H). While the level of LDH release increased after exposure to BAPTA, importantly the levels were the same in uninfected, $\Delta 5$ and $\Delta 5+pYopH$ infected BMPMNs. This result suggests that the differences in IL-10 levels from these cells were not due to differences in cell death. Infection with $\Delta 5+pYopE$ regardless of the presence of calcium flux inhibitors stimulated LDH release indicating that YopE causes PMN cell death. However, since IL-10 was only detected in the supernatant in the absence of calcium flux inhibitors, this is again consistent with the idea that $\Delta 5$ infection stimulates IL-10 production when cells can flux calcium and YopE does not suppress IL-10 production. Collectively, these results demonstrate that YopH inhibits calcium flux and prevents IL-10 production in PMNs.

Discussion

The functions of T3SS effectors have been studied extensively in cell culture models (Alonso et al., 2004; Black et al., 2000; Black et al., 1998; Deleuil et al., 2003; Gerke et al., 2005; Hamid et al., 1999; Yuan et al., 2005). While informative, these cell culture models do not fully recapitulate the interactions between *Yptb* and host cells during infection because cell culture models seldom involve the full array of cells and their activation states that occur in tissues. However, until recently it has been technically difficult to identify the molecular targets of the T3SS effectors during animal infection because there were no good methods for isolating the cells containing effectors. Here we demonstrate a specific signal-transduction pathway targeted by a T3SS effector during animal infection and show that the adapters, PRAM-1, SKAP-HOM and SLP-76 are dephosphorylated in the presence of YopH in PMNs.

This approach is broadly applicable to the study of effectors in animal model systems from pathogens that use T3SS, T4SS or T6SS. Furthermore, both global and focused strategies can be used to uncover the consequences to host cells after injection with different effectors using this system. For instance, effectors from a number of bacterial pathogens, including YopJ from *Yersinia*, target MAPK and NF- κ B pathways (Krachler et al., 2011). To discern their roles in cells from infected tissues, one could examine ubiquitination or phosphorylation patterns of putative targets, monitor pro-inflammatory responses at either the transcriptional or post-transcriptional level, as we have done, and/or evaluate expression of cell surface proteins to assess cell activation states. Global approaches, such as RNASeq, to profile cells injected with different effectors are also very feasible. Finally, when cells are long-lived, the ability of injected cells to perform various functions, such as presenting antigens, could be studied after their isolation. These studies are limited by the number of injected cells recovered, the sensitivity of reagents available to probe for changes, and whether changes within cells are transient or long-lasting. For example, in our case about $2-4 \times 10^4$ TEM^{POS} PMNs were recovered in each spleen. Therefore, we pooled PMNs from several mice for western blot analysis and measurement of cytokine protein levels. Despite these constraints, this approach is a significant and powerful step forward in our ability to probe the roles of effectors in animal infection as it permits scrutiny of effector functions in cells from infected tissues.

The dephosphorylation patterns due to YopH from PMNs isolated from infected mice compared to infected BMPMNs were similar but not identical. Differences could result from

the fact that BMPMNs infection was synchronized so that proteins that are transiently dephosphorylated were detected. In addition, recently migrated PMNs from infected spleens may be in different activation states than BMPMNs and therefore may be expressing different proteins that are susceptible to YopH. Our prior knowledge of YopH targets greatly facilitated the identification of SLP-76. In the absence of such knowledge, the bands could have been identified by infecting mice with a substrate-trapping, catalytically inactive form of YopH, YopHC403A (Black et al., 2000), followed by co-immunoprecipitation with antibody to YopH and either western blotting with antibody to putative targets or mass spec analysis. While we have not definitively identified the ~55kDa detected in PMNs isolated from infected spleens, we think it is SKAP-HOM based on our finding that SKAP-HOM was dephosphorylated in BMPMNs. We hypothesize that the 160kDa band may be PLC 2 (147kDa) or a DOCK, the ~120kDa band may be Vav (98kDa), PRAM-1 (100kDa), CASL (120kDa), Pyk2 (120) or FAK (130kDa) while the ~200kDa protein could be a DOCK.

The steps required for signaling downstream of integrin and immunoreceptor engagement have been studied far less intensively in PMNs than in B and T cells (Fig S2) (Jordan and Koretzky, 2010; Newbrough et al., 2003). Nonetheless, many of the same proteins or their homologs relay signals from receptors to mount PMN-specific responses to pathogens (Brinkmann et al., 2004; Newbrough et al., 2003). Our findings that SKAP-HOM, PRAM-1, SLP-76, PLC 2 and Vav1 are all dephosphorylated in the presence of YopH could result from one of several scenarios (Fig 7). YopH could target each of these proteins; however, we think this is unlikely because phosphorylation levels of PLC 2 and Vav are restored in BMPMNs after 30 minutes, yet YopH is still present. Alternatively, YopH could target only one or a subset of proteins in this pathway, and thereby disrupt all subsequent phosphorylation events. Either is consistent with our data because SLP-76 and SKAP-HOM complexes are two major signal-transduction hubs that relay information to each other and participate in inside-out and outside-in signaling in other cells (Fig 7 and S2) (Alenghat et al., 2012; Menasche et al., 2007; Togni et al., 2005). While to date there have been no studies on SKAP-HOM in PMNs, PRAM-1 regulates several integrin-dependent functions, including ROI production and degranulation (Clemens et al., 2004). Likewise phosphorylation of SLP-76 is critical for integrin-dependent PMN spreading, degranulation and ROI production (Jordan and Koretzky, 2010). These effects are consistent with previously described phenotypes of YopH in PMNs. Specifically, YopH has been shown to block phagocytosis, calcium fluxes and ROI production in human PMNs (Andersson et al., 1999; Grosdent et al., 2002; Ruckdeschel et al., 1996). Combined, these data indicate that YopH disarms bactericidal effects of PMNs in infected tissues by targeting SLP-76 and/or SKAP-HOM/PRAM-1 thereby blocking phagocytosis, calcium signaling and ROI production.

The observation that YopH reduced IL-10 production in PMNs from infected spleens supports the conclusion that YopH interferes with SLP-76 and PLC 2 activation because activation of PLC 2 induces calcium flux activating NF-AT which drives IL-10 expression (Hogan et al., 2003; Lee et al., 2009). IL-10 production after *Yptb* infection has been previously studied in BMDM and in tissues and serum of infected mice (Auerbuch and Isberg, 2007; McPhee et al., 2012). Consistent with our results, Auerbuch and Isberg found that IL-10 was more strongly induced in *Yptb* infected BMDM in the absence of the T3SS suggesting that one or more Yops suppress its expression. However, McPhee et al., found that IL-10 levels were elevated in sera of mice infected with YopM-expressing strains (McPhee et al., 2012). Furthermore, this YopM-dependent induction of IL-10 is likely critical for *Yptb* infection because growth of *yopM* was partially restored in the absence of IL-10 or when IL-10 was supplied exogenously. These apparent discrepancies could be due to differences in bacterial strains and/or tissues samples used in these studies and requires further study. Down-regulation of IL-10 by YopH in PMNs may be an unintended

consequence of other more proximal SLP-76-regulated events disrupted by YopH. Alternatively, *Yptb* may thrive best in environments when low levels of IL-10 are produced by PMNs, but higher levels emanate from other cell types.

In conclusion, the findings that PMNs are selectively targeted for Yop translocation (Durand et al., 2010) and that PMNs are recruited to the site of *Yptb* infection (Crimmins et al., 2012) suggested that the function of Yops in PMNs is critical for successful colonization. We found that YopH targets the PRAM-1/SKAP-HOM and SLP-76 signal transduction pathways in PMNs. However, because growth of *yopH* was not fully restored in the absence of PMNs, we propose that YopH has additional functions in other cell types that promote *Yptb* survival. Future work is directed at determining all the targets of YopH in PMNs and understanding how the SKAP-HOM/PRAM-1 and SLP-76 pathways collaborate in PMNs.

Materials and Methods

Bacterial strains and Mouse Infections

Strains and plasmids used in this work are listed in Table S1. For mouse infections, strains were grown as described in (Logsdon and Meccas, 2003). For infection of BMDMs, J774 macrophages or HEp-2 cells, strains were grown in Yop inducing conditions in 2xYT + 20mM sodium oxalate and 20mM MgCl₂ for 2 hours at 26°C, shifted to 37°C for 2 hours, and then used to infect cells at a MOI of 50:1 for 5 or 30 min. Strains carrying pBAD plasmids were exposed to 50 mM arabinose prior to the shift to 37°C and throughout the infection.

Female, BALB/c (6–8 weeks old) mice obtained from NCI were challenged IV with 200 cfu of WT-ETEM, 2000 cfu of *yopH*-ETEM or 1000 CFU of *yopE*-ETEM for 5 days except for cell depletion experiments. Different doses were used so that comparable numbers of bacteria and TEM^{POS} cells were recovered. For cell depletions, mice were intraperitoneally injected with 50 µg of the Ly6G (1A8) antibody, which depletes PMNs, or the Gr1 (RB6-8C5) antibody, which depletes PMNs and iMO one day prior to and two days after IV inoculation with an equal mixture of kanamycin-resistant IP2666 WT and *yopH* (~1000 total bacteria). Tissues were harvested 3 days p.i. Depletion with RB6-8C5 results in low levels of PMNs as detected by blood smears and FACS with RB6-8C5 (unpublished results).

Experiments involving animals were performed with approval of The Institutional Animal Care and Use Committee of Tufts University.

PMN sorting, CCF4-AM conversion assays and Western blots

Single-cell suspensions of splenocytes from infected mice were generated and labeled as described (Durand et al., 2010) and incubated for 30 min in the dark at room temperature in media containing 1µg/ml CCF4-AM (Invitrogen), 1.5mM probenecid (Sigma) and 100 µg/ml gentamicin for 30 minutes at 4°C with PECy5-CD11b (eBioscience), and PECy7-Ly6G (1A8) (BD Pharmingen) to isolate PMNs (Ly6G⁺). In experiments described in Fig 3A, Fig 4A, and Fig S4A–B, PE-Cy5Gr1⁺, PE-Cy7CD11b⁺ splenocytes were collected, which contained a ~5:1 ratio of PMNs to iMO. Between 2–4 × 10⁴ TEM^{POS} and TEM^{NEG} PMNs were collected per mouse. Cells were pooled so that ~1 × 10⁵ TEM^{POS} and TEM^{NEG} PMNs were analyzed by western blot. TEM^{NEG} PMNs from uninfected mice were collected as controls.

Cells were lysed in SDS sample buffer and 1 × 10⁵ cell equivalents were resolved on a 10% SDS-PAGE gel and electrotransferred to Immobilon-P for Western blot analysis with the following primary antibodies: anti-phosphotyrosine (4G10, Millipore), phospho-paxillin

Y118, paxillin, SLP-76, phospho-Zap-70 Y319/Syk Y352, phospho-Syk Y525/526, (Cell Signaling) phospho-SLP-76 (Y112, Y128 or Y145) (BD Pharmingen), phospho-Vav Y174 (AbCam), SKAP-HOM (Protein Tech), PRAM-1 (Santa Cruz), anti-mouse IgG-HRP conjugated and anti-rabbit IgG-HRP conjugated.

Western blot quantification

Western blot quantifications were analyzed with Gene Tools from Syngene software as follows. For profile heights, the software scanned down individual lanes (higher to lower molecular weight), assigned Rf values to each detected band, and represented them as histograms (height/area of the band vs Rf value down the lane). The level of phosphorylation for each band is represented as the area under the peak. Lanes were compared by overlapping the histogram graphs. Bands with similar phosphorylation levels will overlap i.e. their peak height and area will be similar, while bands with different phosphorylation levels will have different areas under their respective curves.

BMPMN Isolation

BMPMNs were isolated using a Percoll gradient as follows. RPMI was forced through both femur and tibia bones with a syringe and the solution was passed through a 70µm cell strainer. Cells were pelleted, erythrocytes lysed, resuspended in 1mL of HBSS without calcium or magnesium, applied to a three-step gradient of 55%, 65% and 75% Percoll, and centrifuged at 300xg for 30 min at room temperature without brakes. Cells at the 65%–75% interface were collected and washed with HBSS. PMN purity was more than 95% according to flow cytometry analysis with PECy7-Ly6G antibody.

Immunoprecipitations

5×10^5 or 2×10^6 cells were infected for 5 min (SLP-76) or 30 min (ADAP, PRAM-1 or SKAP-HOM) with WT *Yptb* or *yopH* at a MOI of 50:1. Cells were washed with PBS and then lysed in 200 µl of ice-cold immunoprecipitation buffer (50mM Tris-HCl pH 7.4, 1% NP-40, 1mM EGTA, 150mM NaCl, 1mM Na₃VO₄, 10mM NaF and Complete Protease inhibitor (Sigma)) for 30 min at 4°C. Lysates were centrifuged at 13,000xg for 10 min. Supernatants were incubated for 16h at 4°C with 2µg antibody-coupled with protein G-Sepharose beads. Beads were collected by a brief centrifugation, and washed three times with immunoprecipitation buffer. Immune complexes were heated to 95°C in SDS-PAGE sample buffer for 5 min, and subjected to Western blot analysis.

Intracellular Ca²⁺ Measurements

2×10^5 cells BMPMNs were loaded with 4µM Fura-2 in 96 well plates and placed at 37°C in a SpectraMax M5 plate reader (Molecular Devices). Fluorescence at 340 and 380 nm was recorded every 20 sec. Basal levels were recorded for 2–3 min, PMNs were infected with WT or *yopH* at a MOI of 50:1 for 12 min and then ionomycin was added to each well. For experiments with the phospholipase inhibitor, 1µM of U73122, or its inactive analogue, U73343, were pre-incubated with BMPMNs for 3 min, prior to addition of *Yptb*. Intracellular calcium concentrations were calculated as described in (Gryniewicz et al., 1985).

IL-10 ELISA measurements and LDH released

Calcium flux inhibitors or chelators: 25µM BAPTA-AM, 50µM 2-APB, or 5µM EGTA, were added 30 min before infection. BMPMNs (8×10^4 cells/well) were infected with 5+pBAD, 5+pYopH, or 5+pYopE at MOI of 10:1 for 4h. 100µg/ml gentamicin was added for 12 h before supernatants were collected. IL-10 and LDH levels were determined

using the Mouse IL-10 ELISA Ready –SET-Go kit (eBioscience) or CytoTox 96 Non-Reactive Cytotoxicity Kit (Promega) respectively.

Real Time PCR

Five days p.i. with WT-ETEM, *yopH*-ETEM or *yopE*-ETEM, splenocytes were collected, loaded with CCF4-AM and labeled with CCF4 and PECy7-Ly6G (1A8) to sort TEM^{pos} Ly6G⁺ and TEM^{neg} Ly6G⁺. RNA was isolated using Tri-Reagent according to the manufacturer's instructions. One µg of RNA was transcribed to cDNA using TaqMan Reverse Transcription Reagents (Applied Biosystems). cDNA was amplified with primer sets (Overbergh et al., 2003) for mouse IL-10, TNF- and GAPDH using SYBR PCR master mix (Applied Biosystems) and an ABI PRISM 7900HT detection system according to the manufacturer's instructions. Fold induction of mRNA was determined from the threshold cycle (*C_t*) values normalized for GAPDH expression and to the value derived from the naive controls.

Supplementary Material

Refer to Web version on PubMed Central for supplementary material.

Acknowledgments

We thank members of the Mecsas lab and Steve Bunnell for useful discussions and critical reading of the manuscript. HGR was supported by NIH AI007329, EAD was supported by AI007422, and JM was supported by AI056068.

References

- Alenghat FJ, Baca QJ, Rubin NT, Pao LI, Matozaki T, Lowell CA, Golan DE, Neel BG, Swanson KD. Macrophages require Skap2 and Sirpalpha for integrin-stimulated cytoskeletal rearrangement. *Journal of cell science*. 2012; 125:5535–5545. [PubMed: 22976304]
- Alonso A, Bottini N, Bruckner S, Rahmouni S, Williams S, Schoenberger SP, Mustelin T. Lck dephosphorylation at Tyr-394 and inhibition of T cell antigen receptor signaling by Yersinia phosphatase YopH. *J Biol Chem*. 2004; 279:4922–4928. [PubMed: 14623872]
- Andersson K, Magnusson KE, Majeed M, Stendahl O, Fallman M. Yersinia pseudotuberculosis-induced calcium signaling in neutrophils is blocked by the virulence effector YopH. *Infect Immun*. 1999; 67:2567–2574. [PubMed: 10225922]
- Auerbuch V, Isberg RR. Growth of Yersinia pseudotuberculosis in Mice Occurs Independently of Toll-Like Receptor 2 expression and induction of Interleukin-10. *Infect Immun*. 2007; 75:3561–3570. [PubMed: 17420232]
- Black DS, Bliska JB. Identification of p130Cas as a substrate of Yersinia YopH (Yop51), a bacterial protein tyrosine phosphatase that translocates into mammalian cells and targets focal adhesions. *EMBO J*. 1997; 16:2730–2744. [PubMed: 9184219]
- Black DS, Marie-Cardine A, Schraven B, Bliska JB. The Yersinia tyrosine phosphatase YopH targets a novel adhesion-regulated signalling complex in macrophages. *Cell Microbiol*. 2000; 2:401–414. [PubMed: 11207596]
- Black DS, Montagna LG, Zitsmann S, Bliska JB. Identification of an amino-terminal substrate-binding domain in the Yersinia tyrosine phosphatase that is required for efficient recognition of focal adhesion targets. *Mol Microbiol*. 1998; 29:1263–1274. [PubMed: 9767593]
- Bliska JB, Guan KL, Dixon JE, Falkow S. Tyrosine phosphate hydrolysis of host proteins by an essential Yersinia virulence determinant. *Proc Natl Acad Sci U S A*. 1991; 88:1187–1191. [PubMed: 1705028]
- Brinkmann V, Reichard U, Goosmann C, Fauler B, Uhlemann Y, Weiss DS, Weinrauch Y, Zychlinsky A. Neutrophil extracellular traps kill bacteria. *Science*. 2004; 303:1532–1535. [PubMed: 15001782]

- Carsetti L, Laurenti L, Gobessi S, Longo PG, Leone G, Efremov DG. Phosphorylation of the activation loop tyrosines is required for sustained Syk signaling and growth factor-independent B-cell proliferation. *Cell Signal*. 2009; 21:1187–1194. [PubMed: 19296913]
- Casutt-Meyer S, Renzi F, Schmalzer M, Jann NJ, Amstutz M, Cornelis GR. Oligomeric coiled-coil adhesin YadA is a double-edged sword. *PLoS One*. 2010; 5:e15159. [PubMed: 21170337]
- Clemens RA, Newbrough SA, Chung EY, Gheith S, Singer AL, Koretzky GA, Peterson EJ. PRAM-1 is required for optimal integrin-dependent neutrophil function. *Molecular and cellular biology*. 2004; 24:10923–10932. [PubMed: 15572693]
- Crimmins GT, Mohammadi S, Green ER, Bergman MA, Isberg RR, Meccas J. Identification of MrtAB, an ABC transporter specifically required for *Yersinia pseudotuberculosis* to colonize the mesenteric lymph nodes. *PLoS Pathog*. 2012; 8:e1002828. [PubMed: 22876175]
- Daley JM, Thomay AA, Connolly MD, Reichner JS, Albina JE. Use of Ly6G-specific monoclonal antibody to deplete neutrophils in mice. *Journal of leukocyte biology*. 2008; 83:64–70. [PubMed: 17884993]
- Deleuil F, Mogemark L, Francis MS, Wolf-Watz H, Fallman M. Interaction between the *Yersinia* protein tyrosine phosphatase YopH and eukaryotic Cas/Fyb is an important virulence mechanism. *Cell Microbiol*. 2003; 5:53–64. [PubMed: 12542470]
- Durand EA, Maldonado-Arocho FJ, Castillo C, Walsh RL, Meccas J. The presence of professional phagocytes dictates the number of host cells targeted for Yop translocation during infection. *Cell Microbiol*. 2010; 12:1064–1082. [PubMed: 20148898]
- Geijtenbeek TB, Gringhuis SI. Signalling through C-type lectin receptors: shaping immune responses. *Nature reviews Immunology*. 2009; 9:465–479.
- Gerke C, Falkow S, Chien YH. The adaptor molecules LAT and SLP-76 are specifically targeted by *Yersinia* to inhibit T cell activation. *J Exp Med*. 2005; 201:361–371. [PubMed: 15699071]
- Graham DB, Robertson CM, Bautista J, Mascarenhas F, Diacovo MJ, Montgrain V, Lam SK, Cremasco V, Dunne WM, Faccio R, et al. Neutrophil-mediated oxidative burst and host defense are controlled by a Vav-PLCgamma2 signaling axis in mice. *The Journal of clinical investigation*. 2007; 117:3445–3452. [PubMed: 17932569]
- Grosdent N, Maridonneau-Parini I, Sory MP, Cornelis GR. Role of Yops and adhesins in resistance of *Yersinia enterocolitica* to phagocytosis. *Infect Immun*. 2002; 70:4165–4176. [PubMed: 12117925]
- Grynkiewicz G, Poenie M, Tsien RY. A new generation of Ca²⁺ indicators with greatly improved fluorescence properties. *J Biol Chem*. 1985; 260:3440–3450. [PubMed: 3838314]
- Hamid N, Gustavsson A, Andersson K, McGee K, Persson C, Rudd CE, Fallman M. YopH dephosphorylates Cas and Fyn-binding protein in macrophages. *Microb Pathog*. 1999; 27:231–242. [PubMed: 10502464]
- Harmon DE, Davis AJ, Castillo C, Meccas J. Identification and characterization of small-molecule inhibitors of Yop translocation in *Yersinia pseudotuberculosis*. *Antimicrob Agents Chemother*. 2010; 54:3241–3254. [PubMed: 20498321]
- Hogan PG, Chen L, Nardone J, Rao A. Transcriptional regulation by calcium, calcineurin, and NFAT. *Genes & development*. 2003; 17:2205–2232. [PubMed: 12975316]
- Jordan MS, Koretzky GA. Coordination of receptor signaling in multiple hematopoietic cell lineages by the adaptor protein SLP-76. *Cold Spring Harb Perspect Biol*. 2010; 2:a002501. [PubMed: 20452948]
- Koberle M, Klein-Gunther A, Schutz M, Fritz M, Berchtold S, Tolosa E, Autenrieth IB, Bohn E. *Yersinia enterocolitica* targets cells of the innate and adaptive immune system by injection of Yops in a mouse infection model. *PLoS Pathog*. 2009; 5:e1000551. [PubMed: 19680448]
- Krachler AM, Woolery AR, Orth K. Manipulation of kinase signaling by bacterial pathogens. *The Journal of cell biology*. 2011; 195:1083–1092. [PubMed: 22123833]
- Kulathu Y, Grothe G, Reth M. Autoinhibition and adapter function of Syk. *Immunol Rev*. 2009; 232:286–299. [PubMed: 19909371]
- Lee CG, Kang KH, So JS, Kwon HK, Son JS, Song MK, Sahoo A, Yi HJ, Hwang KC, Matsuyama T, et al. A distal cis-regulatory element, CNS-9, controls NFAT1 and IRF4-mediated IL-10 gene activation in T helper cells. *Molecular immunology*. 2009; 46:613–621. [PubMed: 18962896]

- Logsdon LK, Meccas J. Requirement of the *Yersinia pseudotuberculosis* effectors YopH and YopE in colonization and persistence in intestinal and lymph tissues. *Infect Immun*. 2003; 71:4595–4607. [PubMed: 12874339]
- Marketon MM, DePaolo RW, DeBord KL, Jabri B, Schneewind O. Plague bacteria target immune cells during infection. *Science*. 2005; 309:1739–1741. [PubMed: 16051750]
- McPhee JB, Mena P, Zhang Y, Bliska JB. Interleukin-10 induction is an important virulence function of the *Yersinia pseudotuberculosis* type III effector YopM. *Infect Immun*. 2012; 80:2519–2527. [PubMed: 22547545]
- Menasche G, Kliche S, Chen EJ, Stradal TE, Schraven B, Koretzky G. RIAM links the ADAP/SKAP-55 signaling module to Rap1, facilitating T-cell-receptor-mediated integrin activation. *Molecular and cellular biology*. 2007; 27:4070–4081. [PubMed: 17403904]
- Moog-Lutz C, Peterson EJ, Lutz PG, Eliason S, Cave-Riant F, Singer A, Di Gioia Y, Dmowski S, Kamens J, Cayre YE, et al. PRAM-1 is a novel adaptor protein regulated by retinoic acid (RA) and promyelocytic leukemia (PML)-RA receptor alpha in acute promyelocytic leukemia cells. *J Biol Chem*. 2001; 276:22375–22381. [PubMed: 11301322]
- Nathan C. Neutrophils and immunity: challenges and opportunities. *Nature reviews Immunology*. 2006; 6:173–182.
- Newbrough SA, Mocsai A, Clemens RA, Wu JN, Silverman MA, Singer AL, Lowell CA, Koretzky GA. SLP-76 regulates Fcγ receptor and integrin signaling in neutrophils. *Immunity*. 2003; 19:761–769. [PubMed: 14614862]
- Overbergh L, Giulietti A, Valckx D, Decallonne R, Bouillon R, Mathieu C. The use of real-time reverse transcriptase PCR for the quantification of cytokine gene expression. *J Biomol Tech*. 2003; 14:33–43. [PubMed: 12901609]
- Persson C, Carballeira N, Wolf-Watz H, Fallman M. The PTPase YopH inhibits uptake of *Yersinia*, tyrosine phosphorylation of p130Cas and FAK, and the associated accumulation of these proteins in peripheral focal adhesions. *EMBO J*. 1997; 16:2307–2318. [PubMed: 9171345]
- Ruckdeschel K, Roggenkamp A, Schubert S, Heesemann J. Differential contribution of *Yersinia enterocolitica* virulence factors to evasion of microbicidal action of neutrophils. *Infect Immun*. 1996; 64:724–733. [PubMed: 8641773]
- Schaller MD. Paxillin: a focal adhesion-associated adaptor protein. *Oncogene*. 2001; 20:6459–6472. [PubMed: 11607845]
- Spinner JL, Cundiff JA, Kobayashi SD. *Yersinia pestis* type III secretion system-dependent inhibition of human polymorphonuclear leukocyte function. *Infect Immun*. 2008; 76:3754–3760. [PubMed: 18490459]
- Togni M, Swanson KD, Reimann S, Kliche S, Pearce AC, Simeoni L, Reinhold D, Wienands J, Neel BG, Schraven B, et al. Regulation of in vitro and in vivo immune functions by the cytosolic adaptor protein SKAP-HOM. *Molecular and cellular biology*. 2005; 25:8052–8063. [PubMed: 16135797]
- Viboud GI, Bliska JB. *Yersinia* outer proteins: role in modulation of host cell signaling responses and pathogenesis. *Annu Rev Microbiol*. 2005; 59:69–89. [PubMed: 15847602]
- Yuan M, Deleuil F, Fallman M. Interaction between the *Yersinia* tyrosine phosphatase YopH and its macrophage substrate, Fyn-binding protein, Fyb. *J Mol Microbiol Biotechnol*. 2005; 9:214–223. [PubMed: 16415594]
- Zhang X, Majlessi L, Deriaud E, Leclerc C, Lo-Man R. Coactivation of Syk kinase and MyD88 adaptor protein pathways by bacteria promotes regulatory properties of neutrophils. *Immunity*. 2009; 31:761–771. [PubMed: 19913447]

Highlights

Yersinia effector YopH targets SLP-76/Vav/PLC 2 in neutrophils from infected tissues

YopH inactivates PRAM-1/SKAP-HOM in neutrophils

YopH blocks calcium flux and IL-10 in neutrophils from infected tissues

Growth of a *yopH* mutant in spleens and liver is restored in absence of neutrophils

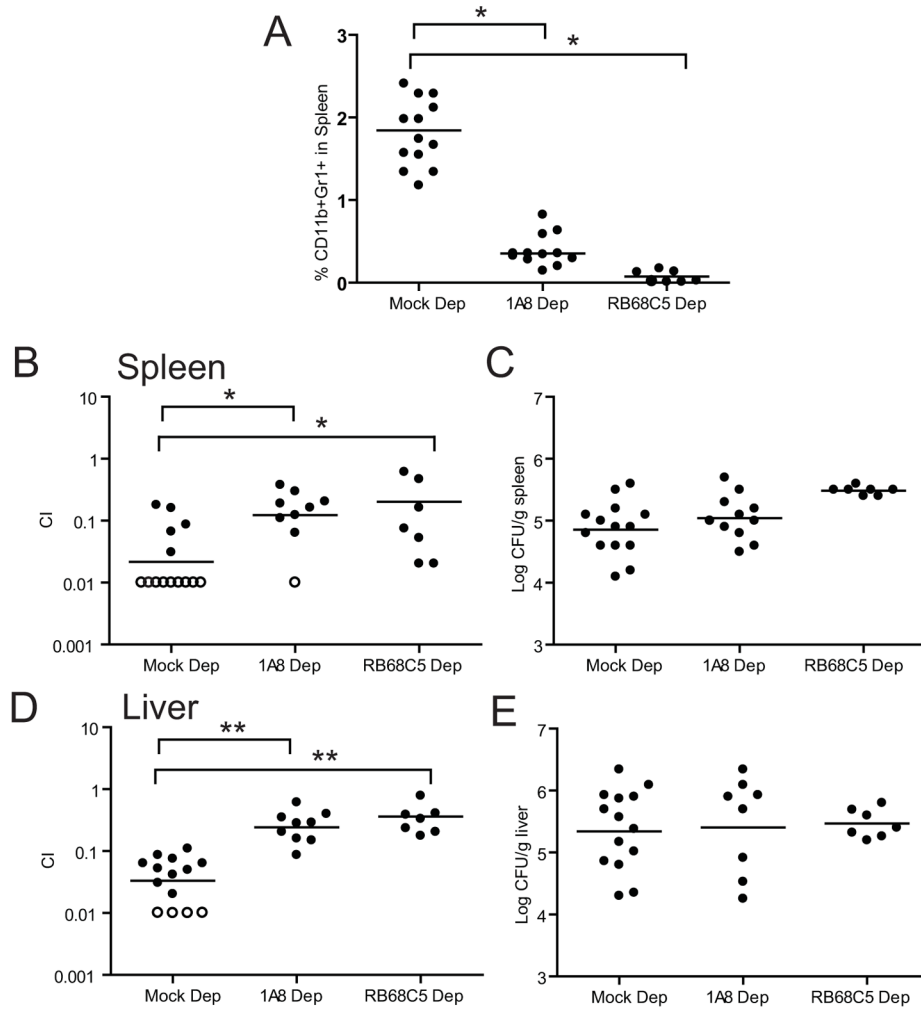


Figure 1. PMN depletion restores growth of a *yopH* strain in competition with WT
 BALB/c were infected IV with an equal mixture of WT-Kan and *yopH* after mock, 1A8 or RB68C5 injection and sacrificed 3 days p.i. (A) Percentage of Gr1⁺CD11b⁺ cells in spleens of untreated mice and mice treated with 1A8 or RB68C5. Competitive index (C.I) in the (B) spleens and (D) livers of BALB/c-depleted mice. The total number of bacteria recovered in the (C) spleen and (E) liver. Each dot represents a mouse; horizontal bars represent the average (A) or geometric mean (B–E); open circles indicate that no *yopH* was recovered in 100 colonies tested. The experiment was repeated twice and all the data is shown. C.I. = (*yopH*/WTKan)_{output} / (*yopH*/WTKan)_{input}. Significance was calculated using one-way ANOVA followed by Tukey’s post test (*P < 0.05 or **P < 0.01). See also Table S1.

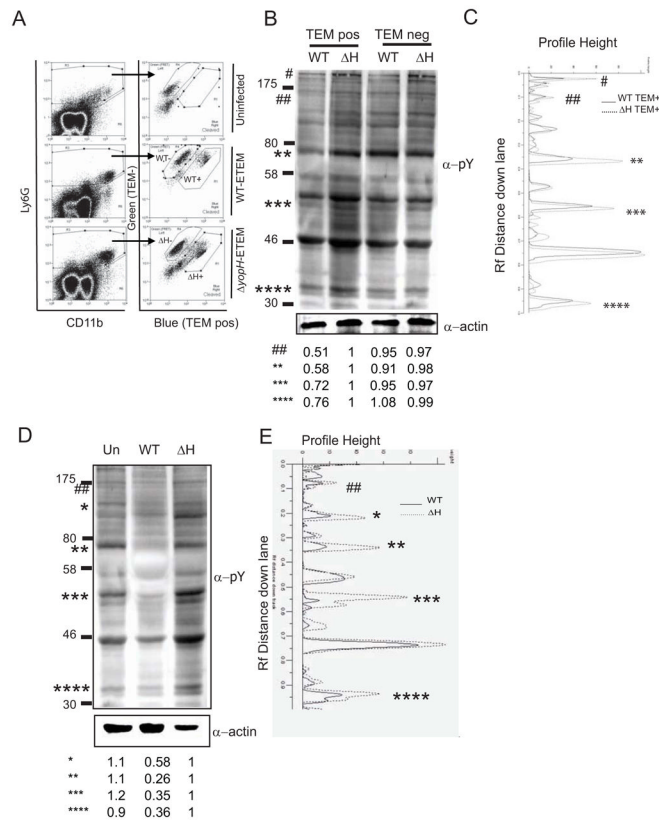


Figure 2. YopH-dependent dephosphorylation in PMNs isolated from spleens of infected animals (A–C) Spleens from mice infected with WT-ETEM or *yopH*-ETEM were harvested 5 days p.i. and TEM^{pos} and TEM^{neg} PMNs were collected. (B–C) Western blot analysis of 1×10^5 TEM^{pos} PMNs and TEM^{neg} PMNs probed with a γ -phosphotyrosine antibody (4G10), stripped and re-probed with α -actin antibody. (D–E) BMPMNs infected with WT or *yopH* strains were lysed and probed with 4G10, stripped and re-probed for actin. (B–E) GeneTools software was used to quantify the phosphorylation levels of bands of interest, denoted by *, by normalizing them to actin controls and then to TEM^{pos} H lane. Each blot is representative of at least 2 independent experiments. * and # denotes bands with reduced intensities; ‘Un’ denotes uninfected PMNs; see also Figure S1.

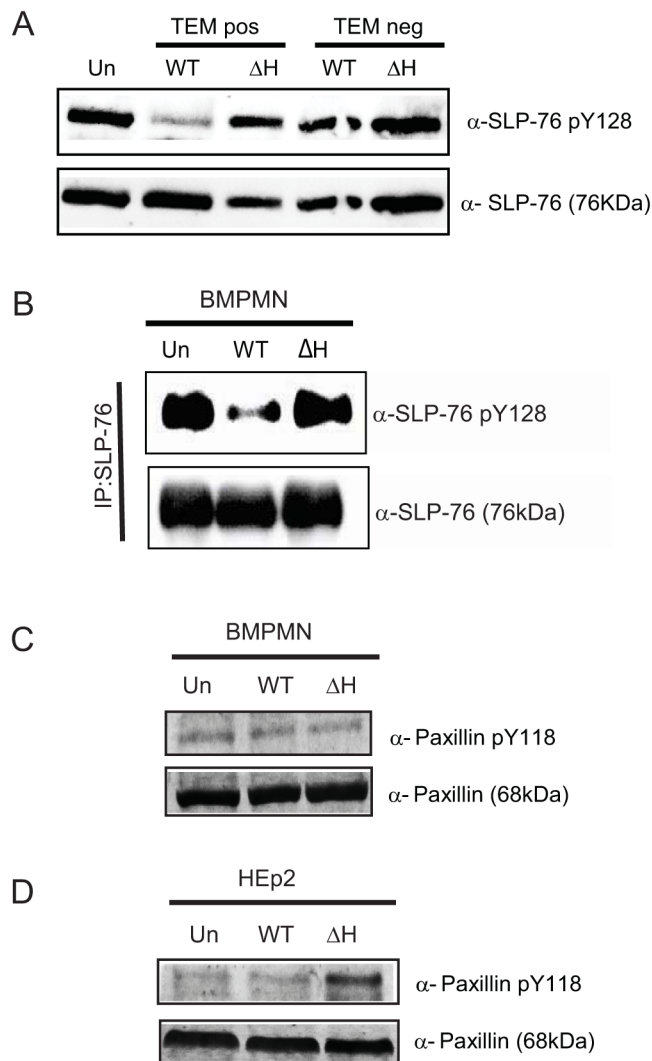


Figure 3. SLP-76, but not paxillin, is dephosphorylated by YopH during animal infection
 (A) TEM^{pos} PMNs and iMo (Gr1⁺CD11b⁺) from mice intravenously infected with WT-E TEM or *yopH*-E TEM for 5 days were collected by FACS. Lysates from 1×10⁵ cells were probed for total SLP-76 and phosphorylation at Y128. (B) BMPMNs (5×10⁵/lane) were infected with WT or *yopH* for 5 min at a MOI of 50:1. Immunoprecipitated SLP-76 was analyzed by Western blot for phosphorylated SLP-76 Y128, and total SLP-76. (C–D) BMPMNs (C) or HEp2 cells (D) were infected at MOI 50:1 for 30 min with WT or *yopH*, lysed and probed for phosphorylation at paxillin Y118 or total paxillin. Blots shown are representative of at least 2 independent experiments; see also Figure S2.

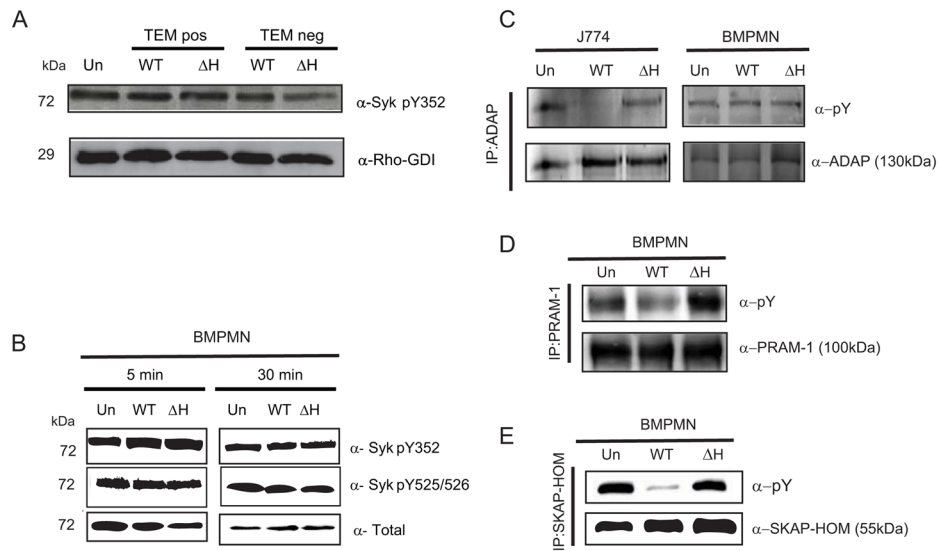


Figure 4. YopH dephosphorylates PRAM-1, SKAP-HOM, but not Syk or ADAP, in PMNs (A)TEM^{pos} Gr1⁺CD11b⁺ and TEM^{neg} Gr1⁺CD11b⁺ PMNs and iMO from spleens of mice infected with WT-E TEM or *yopH*-E TEM for 5 days were collected, lysed and probed for phosphorylation at Y352 in Syk or Rho-GDI as loading control. (B) BMPMNs were infected for 5 or 30 min at a MOI of 50:1 with either WT or *yopH* and then were lysed, resolved by SDS-PAGE and analyzed by Western blot for phosphorylation of Syk pY352, Syk PY525/526 and total. (C) J774 (5×10^5 cells/lane) and BMPMNs (2×10^6 cells/lane) were infected with WT or *yopH* for 30 min at a MOI of 50:1. Lysates were immunoprecipitated with antibodies to ADAP, resolved by SDS-PAGE and analyzed by Western blots for phosphotyrosine and total ADAP. (D–E) BMPMNs (5×10^5 cells/lane) were infected with WT or *yopH* for 30 min at a MOI of 50:1. Lysates were immunoprecipitated with antibodies to PRAM-1 (D) or SKAP-HOM (E), resolved by SDS-PAGE and analyzed by Western blot for phosphotyrosine and total PRAM-1 and SKAP-HOM. All blots shown are representative of at least 2 independent experiments; see also Figures S3.

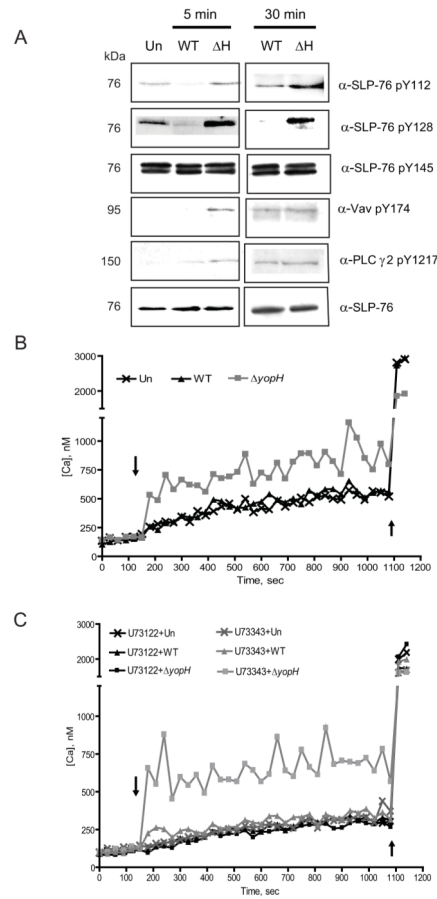


Figure 5. YopH inactivates the SLP-76/Vav/PLC 2 signaling axis and prevents calcium flux in PMNs

(A) BPPMNs were infected for 5 or 30 minutes at a MOI of 50:1 with either WT or *yopH* and then were lysed, resolved by SDS-PAGE and analyzed by Western blot for phosphorylation of SLP-76 pY112, SLP-76 pY128, SLP-76 pY145, Vav-1 pY174, phospho PLC 2, and total SLP-76. All data shown are representative of at least 2 independent experiments. (B–C) BPPMNs were loaded with Fura-2 and (C) with 1 μM U73122 (a PLC inhibitor) or with 1 μM of its inactive analog, U73343. After recording basal levels for 2 (B) or 3 (C) min in a SpectraMax M5 plate reader at 37°C, cells were infected (indicated by the arrow) with WT or *yopH* strains at MOI of 50:1 for 12 min and then ionomycin (indicated by second arrow) was added. Fluorescence was recorded over time to calculate intracellular calcium. Each experiment was repeated three times and a representative experiment is shown.

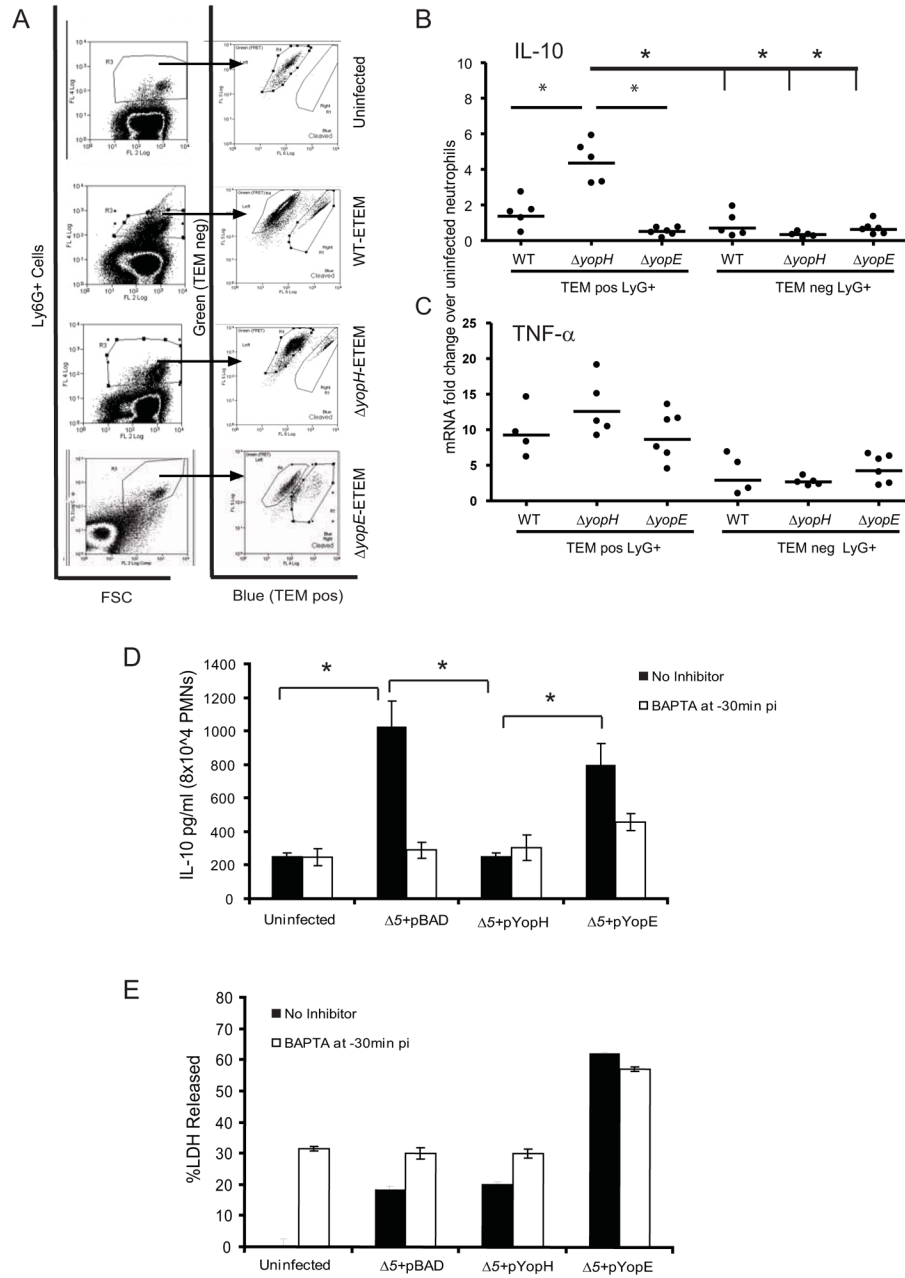


Figure 6. YopH inhibits IL-10 secretion in PMNs

(A–C) Mice were infected IV with either WT-ETEM, *yopH*-ETEM or *yopE*-ETEM for 5 days. TEM^{POS}Ly6G⁺(1A8) and TEM^{NEG}Ly6G⁺(1A8) PMNs from spleens of each mouse were sorted by FACS (A). RNA was isolated and transcript levels of (B) IL-10 and (C) TNF- α were determined using real-time PCR. Each dot represents one animal. (D–E) BMPMNs were untreated or pretreated with 25 μ M BAPTA for 30 minutes and then infected with $\Delta 5+pBAD$, $\Delta 5+pYopH$ or $\Delta 5+pYopE$ at MOI 10:1 for 4 hours before gentamicin was added. The supernatants were collected 12 hours after the addition of gentamicin and IL-10 (D) and LDH (E) levels were determined. Three independent experiments were performed in triplicate. The average \pm STD of one representative experiment is shown. Statistical

significance was calculated using one-way ANOVA with Tukey's post test * indicates $P < 0.05$; see also Figures S4.

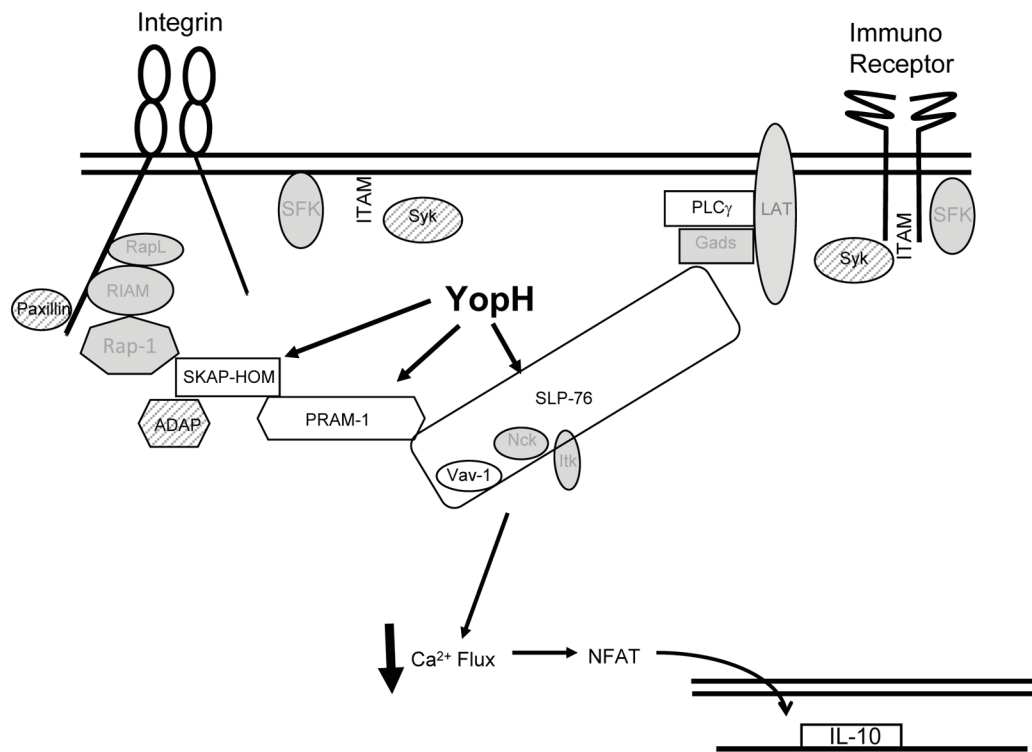


Figure 7. Model of YopH targets in PMNs

YopH targets SLP-76 and/or PRAM-1/SKAP-HOM signal transduction pathways in PMNs. White shapes represent direct or indirect targets of YopH. Calcium flux is blocked and cytokine production altered. Syk, ADAP and paxillin (hatched shapes) were tested, but were not dephosphorylated by YopH in PMNs. Gray shapes represent molecules in pathway not tested.